J Mol Model (2013) 19:521–528
DOI 10.1007/s00894-012-1565-2

ORIGINAL PAPER

Molecular dynamics simulations reveal structural instability of human trypsin inhibitor upon D50E and Y54H mutations

Wanwimon Mokmak · Surasak Chunsrivirot · Anunchai Assawamakin · Kiattawee Choowongkomon · Sissades Tongsima

Received: 5 July 2012 / Accepted: 9 August 2012 / Published online: 7 September 2012

Abstract Serine protease inhibitor Kazal type 1 (SPINK1) plays an important role in protecting the pancreas against premature trypsinogen activation that causes pancreatitis. Various mutations in the SPINK1 gene were shown to be associated with patients with pancreatitis. Recent transfection studies identified intracellular folding defects, probably caused by mutation induced misfolding of D50E and Y54H mutations, as a common mechanism that reduces SPINK1 secretion and as a possible novel mechanism of SPINK1 deficiency associated with chronic pancreatitis. Using molecular dynamics, we investigated the effects of D50E and Y54H mutations on SPINK1 dynamics and conformation at 300 K. We found that the structures of D50E and Y54H mutants were less stable than and were distorted from those of the wild type, as indicated by the RMSD plots, RMSF plots and DSSP series. Specifically, unwinding of the top of helices (the main secondary structures) and the distortion of the loops above the helices were observed. It may be possible that this distorted protein structure may be recognized as "non-native" by members of the chaperone family; it may be further retained and targeted for degradation, leading to SPINK1 secretion reduction and subsequently pancreatitis in patients as Király et al. (Gut 56:1433, 2007) proposed.

Keywords AMBER · DSSP · Molecular dynamics simulations · Pancreatitis · Trypsin inhibitor

Wanwimon Mokmak and Surasak Chunsrivirot contributed equally to this work

Electronic supplementary material The online version of this article (doi:10.1007/s00894-012-1565-2) contains supplementary material, which is available to authorized users.

W. Mokmak · S. Chunsrivirot · A. Assawamakin · S. Tongsima (✉)
National Center for Genetic Engineering and Biotechnology,
113 Thailand Science Park, Phahonyothin Road, Khlong Nueng,
Khlong Luang, Pathum Thani 12120, Thailand
e-mail: sissades@biotec.or.th

W. Mokmak · K. Choowongkomon
Interdisciplinary Graduate Program in Genetic Engineering,
Graduate School, Kasetsart University,
Chatuchak,
Bangkok 10900, Thailand

K. Choowongkomon
Center for Advanced Studies in Tropical Natural Resources,
National Research University-Kasetsart University,
Kasetsart University,
Chatuchak,
Bangkok 10900, Thailand

K. Choowongkomon (✉)
Department of Biochemistry, Faculty of Sciences,
Kasetsart University,
Chatuchak,
Bangkok 10900, Thailand
e-mail: fsciktc@ku.ac.th

Introduction

Trypsin is a pancreatic digestive enzyme that is stored as an inactive precursor named trypsinogen in pancreatic zymogen granules and is strictly controlled under normal conditions to prevent autodigestion of the pancreas. However, in some circumstances excessive activation of trypsinogen to trypsin leads to activation of other zymogens, autodigestion of the pancreas, and subsequently pancreatitis that can be acute or chronic [1]. Believed to play an important role in protecting the pancreas against premature trypsinogen activation [2], serine protease inhibitor Kazal type 1 (SPINK1) is synthesized in acinar cells of the pancreas, and this enzyme can inactivate trypsin activity if trypsinogen is

accidentally converted to trypsin in acinar cells. Mutations in the SPINK1 gene were shown to be associated with patients with pancreatitis by various studies [3–15]. Examples of these mutations are N34S (the relatively common mutation [15]), D50E [9], Y54H [11], R65Q [16], R67C [17–19], and P55S [15].

Acute pancreatitis (AP) is a severe, debilitating and sometimes fatal inflammatory disease. Although the incidence of AP has dramatically increased in recent years, no specific therapy exists [1]. Moreover, chronic pancreatitis is a risk factor for pancreatic ductal adenocarcinoma (PDA) [20, 21] as demonstrated in the cases of hereditary chronic pancreatitis where the incidence of pancreatic cancer in these patients increased by 53 times more than that in the control [22]. Therefore, better understanding in the molecular mechanisms of pancreatitis development may help scientists prevent pancreatitis and pancreatic cancer.

Recent studies by Király et al. [23] identified intracellular folding defects, probably caused by mutation induced misfolding, as a common mechanism that reduces SPINK1 secretion and as a possible novel mechanism of SPINK1 deficiency associated with chronic pancreatitis. They found that D50E and Y54H mutations result in complete loss or marked reduction of SPINK1 secretion, but these mutations did not change trypsin inhibitory activity. They proposed that D50E and Y54H mutations probably cause mutation-induced misfolding that subsequently leads to intracellular retention and degradation of SPINK1. SPINK1 misfolding is most likely caused by the elimination of the conserved hydrogen bond between Asp50 and Tyr54. Therefore, Király et al. proposed that pancreatitis caused by these mutations may join a group of "protein folding disease" such as α1-antitrypsin deficiency and cystic fibrosis [23, 24]. These diseases are known to arise from the conformational instability of an underlying protein, resulting in a change in fold. Recognized as "non-native" by members of the chaperone family, this distorted protein structure is retained and subsequently targeted to a degradative pathway [25]. These structural changes can lead to a decreased level of mature proteins and secretion reduction as well as ordered aggregation and tissue disposition [26].

The objective of this study is to investigate the effects of D50E and Y54H mutations on SPINK1 dynamics and conformation at 300 K. The structures of the wild type, D50E and Y54H mutations were constructed, and three independent simulations for each structure were run at 300 K. DSSP was used to monitor the secondary structures of the wild type and mutants throughout the simulations. The differences in conformational stability and changes in folds of the mutants as compared to the wild type were reported in this article.

Materials and methods

Molecular dynamics simulations

The initial structure of human pancreatic secretory trypsin inhibitor was the crystal structure solved at 2.30 Å (1HPT [27]). The numbering of amino acid residues used in this study was based on that used by Király et al. [23]. The mutations in the crystal structure at position 41, 42, 44 were converted back to amino acid types of the wild type using tools in Discovery Studio 2.5 [28]. All molecular dynamics simulations were performed using the AMBER 10 packages [29, 30] and Amber FF03 force-field parameters [31]. Residues were protonated to correspond to the neutral pH. The structure of the wild-type was solvated with TIP3P water molecules in a truncated octahedron box with a buffer distance of 12 A°. The system was neutralized with Na+ ion, and it was then minimized with the five-step procedure. All five steps of the minimization procedure involved 5000 steepest descent minimization cycles, followed by 5000 conjugate gradient minimization cycles with different restraints on the protein structure. In the first step, the protein coordinates, except hydrogen atoms, were "fixed" at the starting positions using harmonic restraints with a force constant of 5 kcal/(mol · Å^2), while solvent molecules were allowed to relax the unfavorable contacts with other solvent molecules as well as with the solute. For the second, the third and the fourth steps, the backbone of the protein was restrained with harmonic restraints with force constants of 5, 1 and 0.5 kcal/(mol · Å^2), respectively. The last step involves minimization of the entire system with no positional restraints.

Using tools in Discover studios 2.5 [28], the models of D50E and Y54H mutants were created from the minimized structure of wild type by replacing target residues with the desired amino acid. For Y54H mutant, two models, Y54H (δ) and Y54H(ε), were constructed. The delta position of histidine was protonated in Y54H(δ) while the epsilon position of histidine was protonated inY54H(ε). Both models were constructed because hydrogen atoms in the epsilon and delta positions of the histidine residues can both make hydrogen bonds with nearby residues. The structures of the mutants were solvated, neutralize and minimized with the five-step procedure. All systems were heated up from 0 to 300 K during a 500 ps MD simulation run with weak positional restraints on the protein (force constant of 5 kcal/(mol · Å^2)). With no restraints, the systems were further equilibrated at 300 K in the NVT ensemble for 1 ns. The production runs were performed in the NPT ensemble for 50 ns.

The temperature in all simulations was controlled by Langevin dynamics with a collision frequency of 1 ps^{-1}. For NPT simulations, the pressure was maintained at an

average pressure of 1 atm by an isotropic position scaling algorithm with a relaxation time of 2 ps. For every simulation, the random number generator was reseeded [32]. To calculate long-range nonbonded interactions, a cut-off of 12 Å and the particle mesh Ewald method were employed with the default parameters. SHAKE constraints [33] with the tolerance parameter of 10^{-5} Å were employed to eliminate bond-stretching freedom for all bonds involving hydrogen, thereby allowing the use of a 0.002 ps time step.

With different seeding numbers, three independent simulations were performed for the wild-type, D50E, Y54H(δ) and Y54H(ε) models. The C_α root-mean-square deviations (RMSD) and the C_α root mean-square-fluctuations (RMSF) relative to the average MD structure were calculated. The DSSP algorithm [34], as implemented in AMBER, was used to determine the type of secondary structure for each residue.

Results and discussion

Structural deviations

The minimized structure of the wild type is shown in Fig. 1. The main folds of SPINK1 comprise one helix, which are residues 57–67 (H), and three beta sheets, which are residues 46–48 (S1), 53–54 (S2), and 73–76 (S3). Additionally, the wild type has a flexible N-terminus (residues 24–45).

Figure 2 shows the RMS positional deviations, excluding the flexible N-terminals (residue 24–45), from the minimized structure as functions of simulation time for the C_α atoms of the wild type, D50E, Y54H(δ) (delta position was protonated) and Y54H(ε) mutants (epsilon position was protonated) of the first run. The RMSD plots of the second and third runs are shown in Fig. S1 in the supplemental material. The root-mean-square deviation (RMSD) values of the wild type reach plateaus around 0.6–0.7 Å, while those of the mutants (except the third run of D50E) reach plateaus at higher RMSD values (around 1.0–1.2 Å) due to structural changes. This result may suggest that the conformations of the mutants underwent conformational changes at a higher degree than those of the wild type.

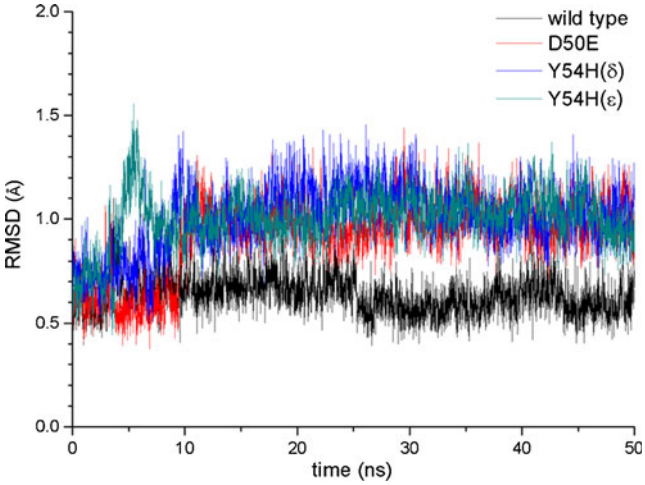

Fig. 2 RMSD of wild type, D50E, Y54H(δ), Y54H(ε) mutants (excluding the flexible N-terminals)

The root-mean-square fluctuation (RMSF) plot of C_α atoms of the wild type, D50E, Y54H(δ) and Y54H(ε) mutants of the first run are shown in Fig. 3. The RMSF plots of the second and third runs are shown in Fig. S2 in the supplemental material. The RMSF values of the loops and the N-terminals, especially residues 24 and 25, are higher

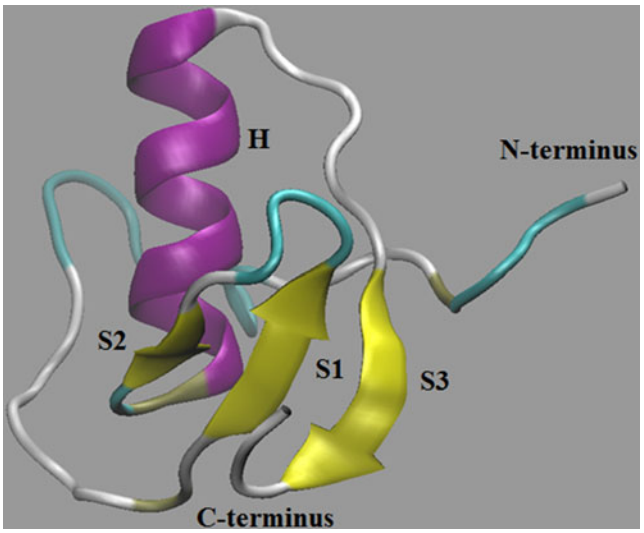

Fig. 1 Ribbon diagram showing secondary structures of wild-type SPINK1. Helix is shown in purple and sheets are shown in yellow

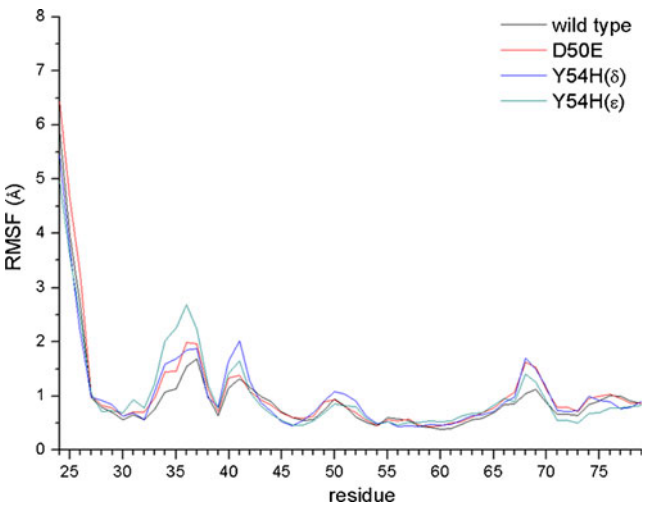

Fig. 3 RMS fluctuation of wild type, D50E, Y54H(δ), Y54H(ε) mutants

than other residues due to their flexibilities. On average, the RMSF values of the mutants are higher than those of the wild type, especially the RMSF values of residues 67–69 (top of helix H and the loop connecting to it). The increase of fluctuations and dynamics during the simulations may suggest the decreased stability of the mutants, as compared to the wild type.

Changes in secondary-structures

As determined by DSSP algorithm, Fig. 4 shows the evolution of the secondary structures during the simulation of the first run. The DSSP series of the second and third runs are displayed in Fig. S3 in the supplemental material. The secondary-structure assignments of the crystal structure given by Hecht et al. [27] are depicted at the left margins of the DSSP series. Generally, the DSSP classification are largely in agreement with the secondary-structure assignments of the crystal structure given by Hecht et al. [27]. The exceptions are residue 28, where it was marked as anti-parallel beta sheet by DSSP while it was assigned to be coil by Hecht et al., and residue 74, where it was marked as coil by DSSP and assigned to be anti-parallel beta sheet by Hecht et al.

The overall structures of the wild type remain roughly intact throughout the 50 ns simulations. Some fluctuations were observed at the top and bottom helix H, switching between alpha helix (blue) and turn (yellow) at the top and between alpha helix (blue) and coil (white) at the bottom. Fluctuations were also observed at the top and/or bottom of the anti-parallel beta sheets S1, S2 and S3. They fluctuate between anti-parallel (red) and turn (yellow) or between anti-parallel (red) and coil (white). Some residues next to the beta sheets such as residues 44, 45, 52, 72, and 77 also show fluctuations between anti-parallel (red) and coil (white).

However, major structural changes of the D50E, Y54H (δ) and Y54H(ε) mutants were observed from the DSSP series. Specifically, the top of helix H (especially at residue 67) of the mutants were unwound as indicated by the disappearance of the blue color at residue 67, and the structures of the loops (residue 68–72) on top of helices H of the mutants were also distorted upward as compared to those of the wild type. The structures of the wild type and mutants after 50 ns simulation of the first run are shown in Figs. 5 and 6. The structures of the second and third runs are shown in Figs. S4, S5, S6 and S7 in the supplemental material, respectively. For comparison, the structures of the wild type after minimization are also displayed in Fig. 7. Similar to the

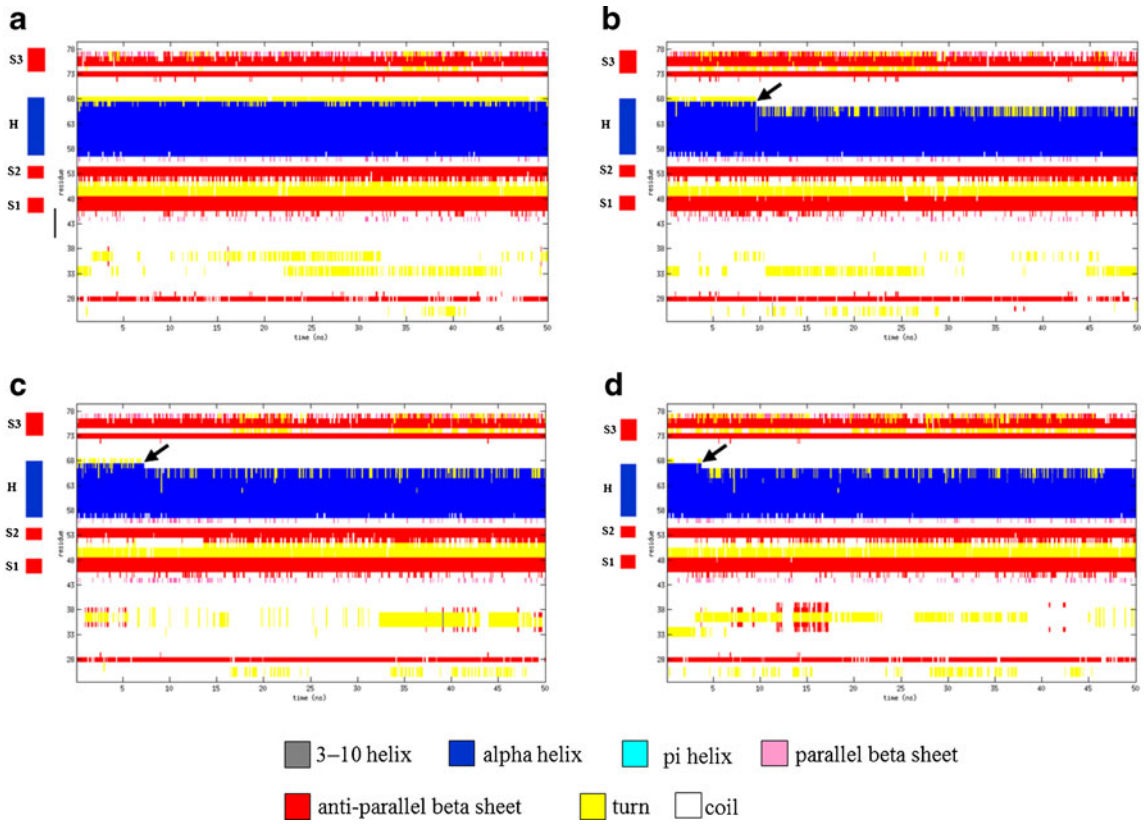

Fig. 4 Secondary structure as a function of simulation time (as determine by DSSP). The arrows indicate the points where helices H start to unwind. (**a**) wild type, (**b**) D50E, (**c**) Y54H(δ), (**d**) Y54H(ε)

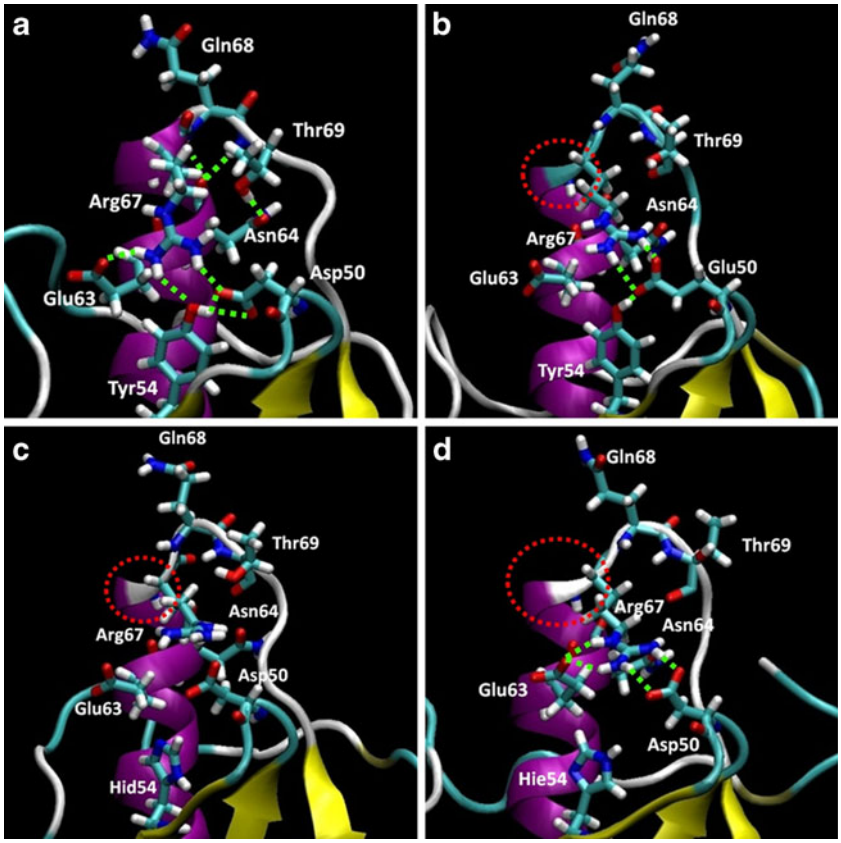

Fig. 5 Front views of the structures of the wild type and mutants after 50 ns simulations. Important residues are shown in licorice. Unwinding of the top of the main helices H is circled in red. Important hydrogen bonds are shown as green dashed lines. (**a**) wild type, (**b**) D50E, (**c**) Y54H(δ), (**d**) Y54H (ε)

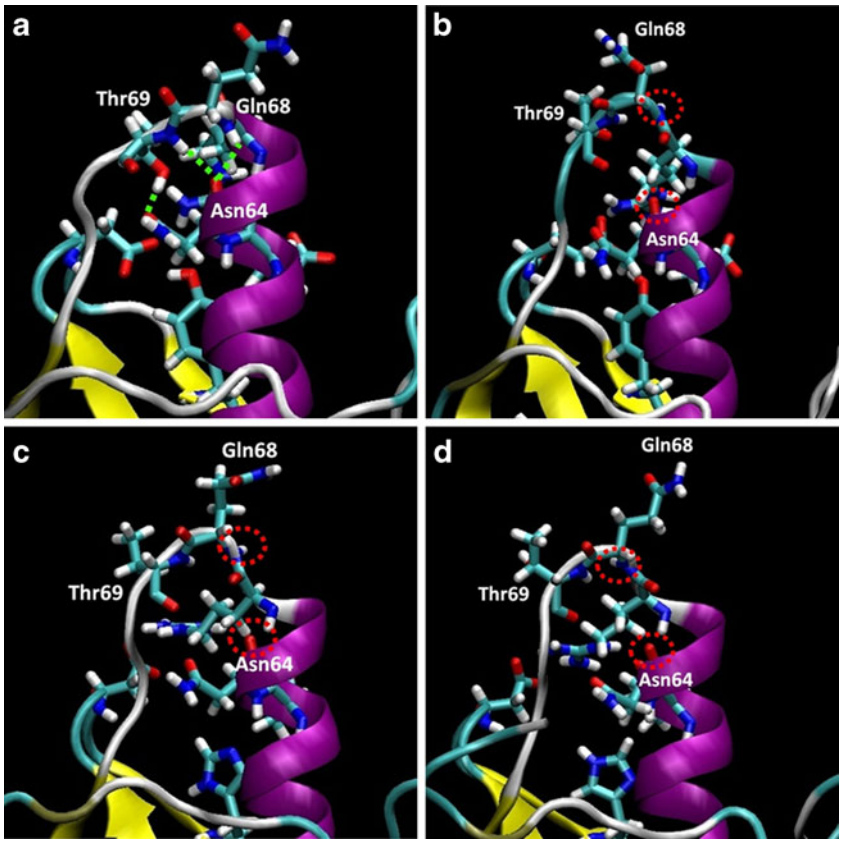

Fig. 6 Back views of the structures of the wild type and mutants after 50 ns simulations. Important residues are shown in licorice. Important hydrogen bonds are shown as green dashed lines. The absences of hydrogen bonds between the backbone carbonyl oxygens of Asn64 and the backbone amino hydrogens of Gln68 are circled in red. (**a**) wild type, (**b**) D50E, (**c**) Y54H(δ), (**d**) Y54H(ε)

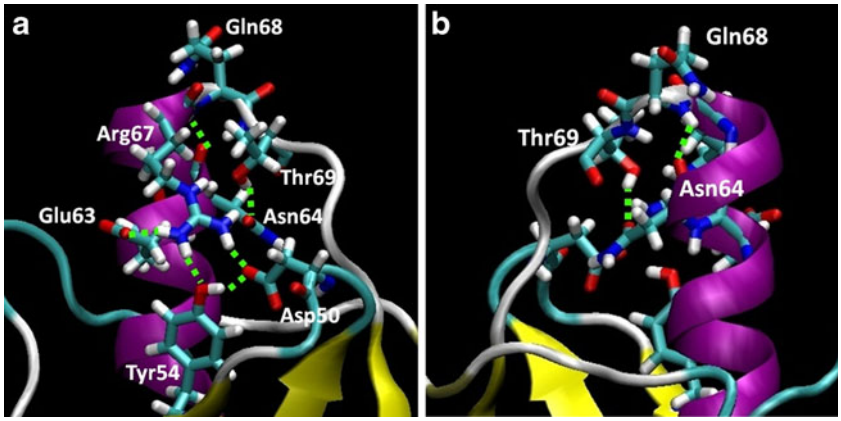

Fig. 7 The structures of the wild type after minimization. Important residues are shown in licorice. Important hydrogen bonds are shown as green dashed lines. (**a**) front, (**b**) back

wild type, some fluctuations were observed in the D50E, Y54H(δ) and Y54H(ε) mutants at the top and/or bottom of the anti-parallel beta sheets S1, S2 and S3. They switched between anti-parallel (red) and turn (yellow) or between anti-parallel (red) and coil (white). Fluctuations between anti-parallel (red) and coil (white) of some residues next to the beta sheets were also observed.

Unwinding of helix H and distortion of the loop on top of helix H of each mutant are probably caused by the loss of the important hydrogen bond at the top of helix H between the backbone carbonyl oxygen of Asn64 and the backbone amino hydrogen of Gln68. Figure 8 shows the hydrogen bond distance profiles of the backbone carbonyl oxygen of Asn64 and the backbone amino hydrogen of Gln68 of the wild type and mutants of the first run. The hydrogen bond distance profiles of the second and third runs are shown in Fig. S8 in the supplemental material. The time points, where the hydrogen bond distances drastically increase (indicating the loss of hydrogen bonds), agree well with the time points where unwinding of helices H occur in the DSSP series (Figs. 4 and S3). These results support the importance of the hydrogen bond between the backbone carbonyl oxygen of Asn64 and the backbone amino hydrogen of Gln68 to structural integrity of helix H.

In the wild type, this hydrogen bond is maintained by the intricate hydrogen bond networks formed by Tyr54, Asp50,

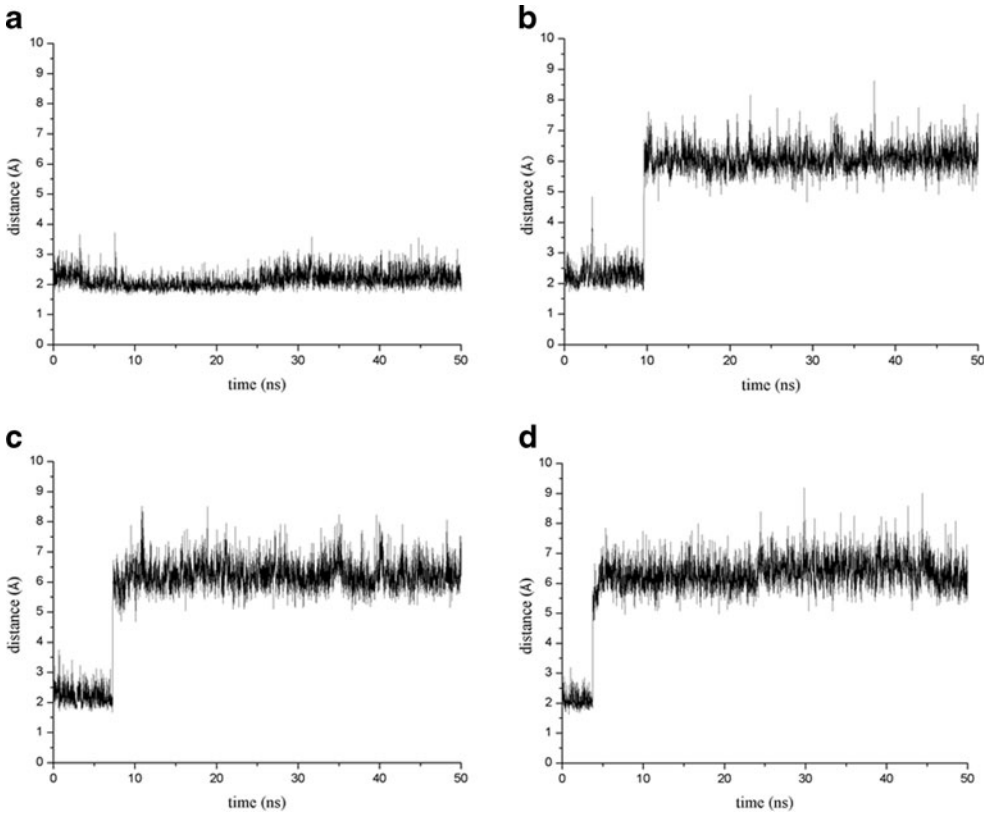

Fig. 8 Hydrogen bond distance profiles between backbone oxygen of the carbonyl group of Asn64 and backbone hydrogen of the amino group of Gln 68. (**a**) wild type, (**b**) D50E, (**c**) Y54H(δ), (**d**) Y54H(ε)

Arg67, Glu63, Thr69 and Asn64 (Figs. 5, 6 and 7). Specifically, the formation of the backbone hydrogen bond between Asn64 and Gln68 is provided by a suitable orientation and position of Gln68, which is on the loop on top of helix H. A suitable orientation and position of the backbone of Gln68 is maintained by a hydrogen bond between Thr69, which is on the loop on top of helix H, and Asn64, which is on helix H, as well as the rigidity of Arg67, which is next to Gln68. The rigidity of Arg67 is maintained by the hydrogen bonds between Arg67 and three other residues (Asp50, Tyr54, Glu63).

The mutations of Tyr54 or Asp50 to other residue disturb these intricate hydrogen bond networks, and increase the fluctuation of Arg67 and nearby residues in the loop on top of helix H, as indicated by the RMSF plot (Fig. 3). Due to the increased fluctuation, Thr69 gradually loses a hydrogen bond with Asn64, which helps maintain the position of the loop on top of helix H. As a result, the backbone amino hydrogen of Gln68 gradually moves away from the backbone carbonyl oxygen of Asn64, resulting in unwinding of the top of helix H and distortion of the loop on top of helix H (Fig. 9).

The conformations of the three independent runs of each protein largely confirm our proposed hypothesis, except for the third run of D50E, where the decay of helix H was not observed. This discrepancy could occur due to the fact that the mutation from Asp to Glu is not as drastic as Tyr to His. Asp and Glu have the same carboxyl group but Glu has one extra methylene group. On the other hand, the mutation from Tyr to His is the drastic change in functional groups as well as the length and the size of the side chains. Tyr contains a tyrosyl group, which has phenyl and hydroxyl groups, while His contains a histidyl group, which has an imidazole group. Therefore, the probability that the D50E mutation will disrupt the hydrogen bond network that keeps the helix H intact may be lower than those of Y54H(δ) and Y54H(ε) mutations.

For the three independent runs of Y54H(δ) and another three runs of Y54H(ε), although the protonation positions of Y54H(δ) and Y54H(ε) are different, the results are quite similar; unwinding of the top of helices H and distortions of the loops at the top of the helices were observed. These findings suggest that, regardless of the protonation positions, Y54H is a drastic mutation that disrupts important hydrogen bond networks that subsequently causes instability, helix decay and distortion of the loop on top of the helix.

As previously mentioned, Király et al. [23] identified D50E and Y54H mutations to cause mutation-induced misfolding that may ultimately cause pancreatitis. The misfolding does not change trypsin inhibitory activity but it is sufficient to be targeted by chaperones to a degradative pathway. Therefore, the structural changes of such misfolding should be subtle. Our results from the 50 ns simulations of the D50E and Y54H mutants show these subtle structural changes, partial unwinding of the top of the helix H and the distortion of the loop above the helix. It may be possible that this distorted protein structure may be recognized as "non-native" by members of the chaperone family; this distorted protein may be further retained and targeted for degradation, leading to SPINK1 secretion reduction and subsequently pancreatitis in patients as Király et al. [23] proposed.

Conclusions

To investigate the effects of D50E and Y54H mutations on SPINK1 dynamics and conformation, the structures of the wild type, D50E, Y54H(δ) and Y54H(ε) mutations were constructed, and three independent simulations for each structure were run at 300 K. We found that the structures of the mutants were less stable than those of the wild type as indicated by the RMSD plots, RMSF plots and DSSP series. Moreover, their structures were distorted from those of the wild type. Specifically, the unwinding of the top of helices H (the main secondary structures) and the distortions of the loops on top of helices H of the mutants were observed. There is a possibility that these distorted protein structures may be recognized as "non-native" by members of the chaperone family; they may be further retained and targeted for degradation, resulting in SPINK1 secretion reduction and subsequently pancreatitis in patients as Király et al. [23] proposed.

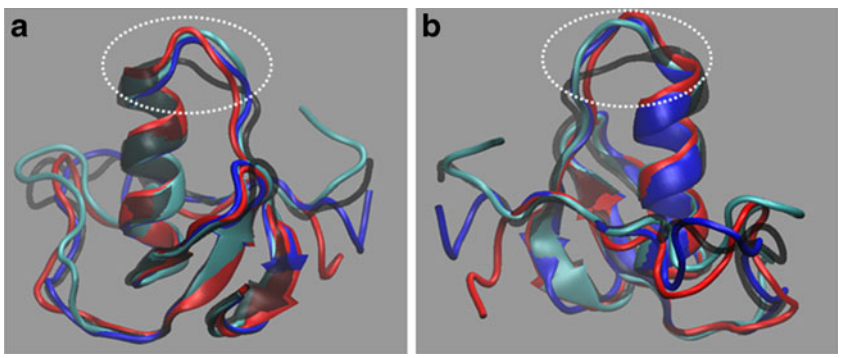

Fig. 9 Superimposition of the structures of the wild type and mutants after 50 ns simulations. Unwinding of the top of helices H and the distortions of the loops above helices H are circled in white. Wild type is colored and shown in transparent black. D50E, Y54H (δ), and Y54H(ε) are colored in red, blue and cyan, respectively. (**a**) front, (**b**) back

Acknowledgments The authors would like to thank the National Center for Genetic Engineering and Biotechnology (BIOTEC) and the National Science and Technology Development Agency (NSTDA) for the use of high performance computer clusters. The National Nanotechnology Center (NANOTEC) for the use of Discovery Studio. Mr. Chumpol Ngamphiw for his technical supports on the clusters. Mr. Pongsakorn Wangkumhang and Mr. Supasak Kulawonganunchai for helpful technical discussions. This work was supported by the Office of the Higher Education Commission and Mahidol University under the National Research Universities Initiative, the Thailand Research Fund (TRF) under Project no. RSA5480026, the "Research Chair Grant" National Science and Technology Development Agency, and the Higher Education Research Promotion and National Research University Project of Thailand, the Office of the Higher Education Commission.

References

1. Ohmuraya M, Yamamura K (2011) The roles of serine protease inhibitor kazal type 1 (spink1) in pancreatic diseases. Exp Anim Tokyo 60:433–444
2. Rinderknecht H (1986) Activation of pancreatic zymogens. Digest Dis Sci 31:314–321
3. Bhatia E, Choudhuri G, Sikora SS, Landt O, Kage A, Becker M, Witt H (2002) Tropical calcific pancreatitis: strong association with spink1 trypsin inhibitor mutations. Gastroenterology 123:1020–1025
4. Chandak G, Idris M, Reddy D, Bhaskar S, Sriram P, Singh L (2002) Mutations in the pancreatic secretory trypsin inhibitor gene (psti/spink1) rather than the cationic trypsinogen gene (prss1) are significantly associated with tropical calcific pancreatitis. J Med Genet 39:347–351
5. Chen JM, Mercier B, Audrezet MP, Raguenes O, Quere I, Ferec C (2001) Mutations of the pancreatic secretory trypsin inhibitor (psti) gene in idiopathic chronic pancreatitis. Gastroenterology 120:1061
6. Drenth J, Te Morsche R, Jansen J (2002) Mutations in serine protease inhibitor kazal type 1 are strongly associated with chronic pancreatitis. Gut 50:687
7. Hassan Z, Mohan V, Ali L, Allotey R, Barakat K, Faruque MO, Deepa R, McDermott MF, Jackson AE, Cassell P (2002) *SPINK1* is a susceptibility gene for fibrocalculous pancreatic diabetes in subjects from the indian subcontinent. Am J Hum Genet 71:964–968
8. Noone PG, Zhou Z, Silverman LM, Jowell PS, Knowles MR, Cohn JA (2001) Cystic fibrosis gene mutations and pancreatitis risk: relation to epithelial ion transport and trypsin inhibitor gene mutations. Gastroenterology 121:1310–1319
9. Pfützer RH, Barmada MM, Brunskill APJ, Finch R, Hart PS, Neoptolemos J, Furey WF, Whitcomb DC (2000) Spink1/psti polymorphisms act as disease modifiers in familial and idiopathic chronic pancreatitis. Gastroenterology 119:615–623
10. Plendl H, Siebert R, Steinemann D, Grote W (2001) High frequency of the n34s mutation in the spink1 gene in chronic pancreatitis detected by a new pcr–rflp assay. Am J Med Genet 100:252–253
11. Schneider A, Suman A, Rossi L, Barmada MM, Beglinger C, Parvin S, Sattar S, Ali L, Khan A, Gyr N (2002) Spink1/psti mutations are associated with tropical pancreatitis and type ii diabetes mellitus in bangladesh. Gastroenterology 123:1026–1030
12. Threadgold J, Greenhalf W, Ellis I, Howes N, Lerch M, Simon P, Jansen J, Charnley R, Laugier R, Frulloni L (2002) The n34s mutation of spink1 (psti) is associated with a familial pattern of idiopathic chronic pancreatitis but does not cause the disease. Gut 50:675
13. Truninger K, Witt H, Köck J, Kage A, Seifert B, Ammann RW, Blum HE, Becker M (2002) Mutations of the serine protease inhibitor, kazal type 1 gene, in patients with idiopathic chronic pancreatitis. Am J Gastroenterol 97:1133–1137
14. Weiss FU, Simon P, Bogdanova N, Mayerle J, Dworniczak B, Horst J, Lerch MM (2005) Complete cystic fibrosis transmembrane conductance regulator gene sequencing in patients with idiopathic chronic pancreatitis and controls. Gut 54:1456
15. Witt H, Luck W, Hennies HC, Claßen M, Kage A, Laß U, Landt O, Becker M (2000) Mutations in the gene encoding the serine protease inhibitor, kazal type 1 are associated with chronic pancreatitis. Nat Genet 25:213–216
16. Ockenga J, Dork T, Stuhrmann M (2001) Low prevalence of spink1 gene mutations in adult patients with chronic idiopathic pancreatitis. J Med Genet 38:243–244
17. Hirota M, Kuwata K, Ohmuraya M, Ogawa M (2003) From acute to chronic pancreatitis: the role of mutations in the pancreatic secretory trypsin inhibitor gene. JOP 4:83–88
18. Kuwata K, Hirota M, Nishimori I, Otsuki M, Ogawa M (2003) Mutational analysis of the pancreatic secretory trypsin inhibitor gene in familial and juvenile pancreatitis in japan. J Gastroenterol 38:365–370
19. Kuwata K, Hirota M, Sugita H, Kai M, Hayashi N, Nakamura M, Matsuura T, Adachi N, Nishimori I, Ogawa M (2001) Genetic mutations in exons 3 and 4 of the pancreatic secretory trypsin inhibitor in patients with pancreatitis. J Gastroenterol 36:612–618
20. Lowenfels AB, Maisonneuve P, Cavallini G, Ammann RW, Lankisch PG, Andersen JR, Dimagno EP, Andren-Sandberg A, Domellof L (1993) Pancreatitis and the risk of pancreatic cancer. New Engl J Med 328:1433–1437
21. Malka D, Hammel P, Maire F, Rufat P, Madeira I, Pessione F, Levy P, Ruszniewski P (2002) Risk of pancreatic adenocarcinoma in chronic pancreatitis. Gut 51:849
22. Lowenfels AB, Maisonneuve P, DiMagno EP, Elitsur Y, Gates LK Jr, Perrault J, Whitcomb DC (1997) Hereditary pancreatitis and the risk of pancreatic cancer. J Natl Cancer Inst 89:442–446
23. Király O, Wartmann T, Sahin-Tóth M (2007) Missense mutations in pancreatic secretory trypsin inhibitor (spink1) cause intracellular retention and degradation. Gut 56:1433
24. Chaudhuri TK, Paul S (2006) Protein–misfolding diseases and chaperone–based therapeutic approaches. FEBS J 273:1331–1349
25. Welch WJ (2004) Role of quality control pathways in human diseases involving protein misfolding. Semin Cell Dev Biol 15:31–38
26. Carrell RW, Gooptu B (1998) Conformational changes and disease—serpins, prions and alzheimer's. Curr Opin Struc Biol 8:799–809
27. Hecht H, Szardenings M, Collins J, Schomburg D (1992) Three-dimensional structure of a recombinant variant of human pancreatic secretory trypsin inhibitor (kazal type). J Mol Biol 225:1095–1103
28. Accelrys Inc. Discovery studio 2.5 package, San Diego, CA
29. Case DA, Cheatham TE III, Darden T, Gohlke H, Luo R, Merz KM Jr, Onufriev A, Simmerling C, Wang B, Woods RJ (2005) The amber biomolecular simulation programs. J Comput Chem 26:1668–1688
30. Case DA, Darden TA, Cheatham TE III, Simmerling C, Wang J (2008) Amber 10, San Francisco
31. Duan Y, Wu C, Chowdhury S, Lee MC, Xiong G, Zhang W, Yang R, Cieplak P, Luo R, Lee T (2003) A point–charge force field for molecular mechanics simulations of proteins based on condensed–phase quantum mechanical calculations. J Comput Chem 24:1999–2012
32. Cerutti DS, Duke R, Freddolino PL, Fan H, Lybrand TP (2008) A vulnerability in popular molecular dynamics packages concerning langevin and andersen dynamics. J Chem Theor Comput 4:1669–1680
33. Ryckaert JP, Ciccotti G, Berendsen HJC (1977) Numerical integration of the cartesian equations of motion of a system with constraints: molecular dynamics of *n*-alkanes. J Comput Phys 23:327–341
34. Kabsch W, Sander C (1983) Dictionary of protein secondary structure: pattern recognition of hydrogen–bonded and geometrical features. Biopolymers 22:2577–2637